The Abdus Salam
International Centre for Theoretical Physics

United Nations
Educational, Scientific
and Cultural Organizat

International Atomic
Energy Agency

SMR.1670 - 29

INTRODUCTION TO MICROFLUIDICS

8 - 26 August 2005

Chip-based IR and Raman Spectroscopy

H. Gardeniers
University of Twente, Enschede, The Netherlands

Chip-based IR and Raman spectroscopy

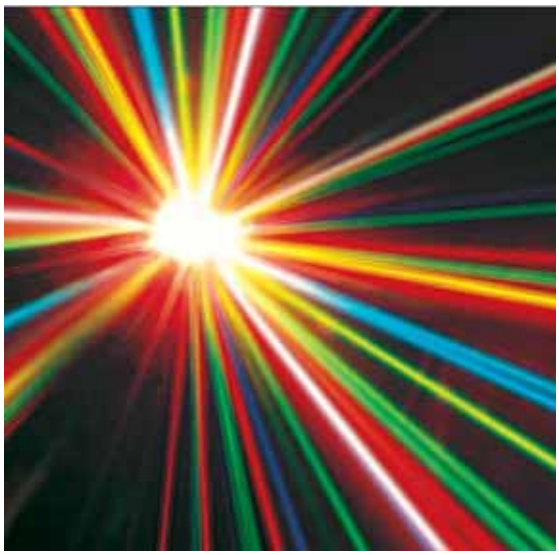

Han Gardeniers
MESA+ Institute for Nanotechnology
University of Twente

Summer School in Microfluidics
ICTP, Trieste, Italy

InfraRed basics

Region	Wavelength range (μm)	Wavenumber range (cm^{-1})
Near	0.78 - 2.5	12800 - 4000
Middle	2.5 - 50	4000 - 200
Far	50 - 1000	200 - 10

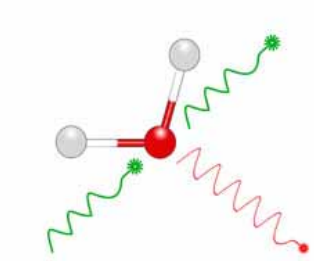

(wavenumber = 1 / wavelength in centimeters)

The most useful IR region is between 4000 - 670 cm^{-1}

IR radiation interacts with vibrational and rotational states of molecules, in case the vibrations or rotations cause a net change in the dipole moment of the molecule.
Rotational transitions are only visible for gases, in liquids or solids, the corresponding IR lines broaden into a continuum due to molecular collisions and other interactions.

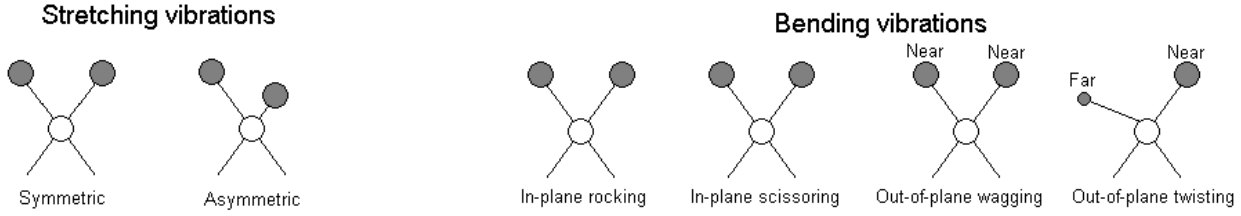

Change in inter-atomic distance along bond axis

Change in angle between two bonds.

source: http://www.shu.ac.uk/schools/sci/chem/tutorials/molspec/irspec1.htm

InfraRed basics

In addition to the vibrations mentioned above, interaction between vibrations can occur (coupling) if the vibrating bonds are joined to a single, central atom. Vibrational coupling is influenced by a number of factors:

•Strong coupling of stretching vibrations occurs when there is a common atom between the two vibrating bonds

•Coupling of bending vibrations occurs when there is a common bond between vibrating groups

•Coupling between a stretching vibration and a bending vibration occurs if the stretching bond is one side of an angle varied by bending vibration

•Coupling is greatest when the coupled groups have approximately equal energies

•No coupling is seen between groups separated by two or more bonds

source: http://www.shu.ac.uk/schools/sci/chem/tutorials/molspec/irspec1.htm

Fourier-Transform IR

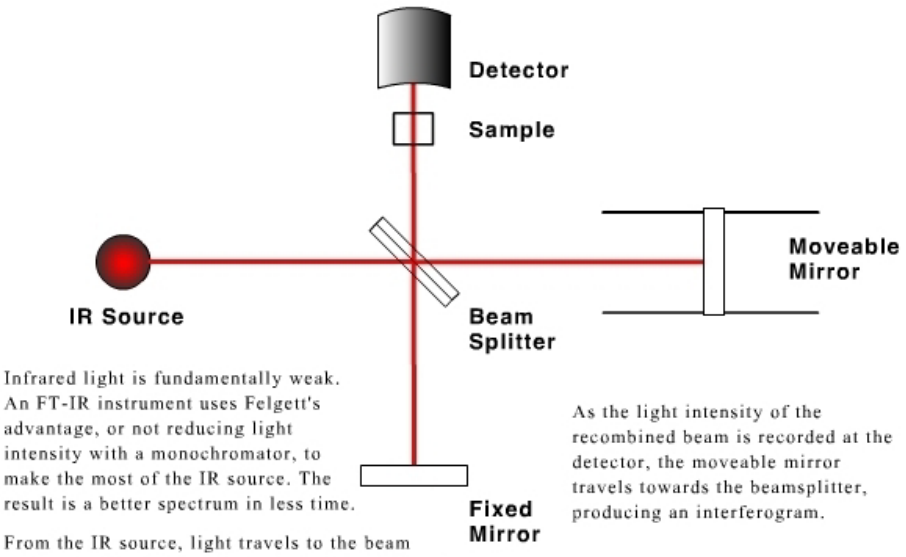

Infrared light is fundamentally weak. An FT-IR instrument uses Felgett's advantage, or not reducing light intensity with a monochromator, to make the most of the IR source. The result is a better spectrum in less time.

From the IR source, light travels to the beam splitter. 50% of the light is reflected to the fixed mirror and 50% is transmitted to the moveable mirror. Light travels to each of the mirrors and recombines at the beam splitter before passing through the sample and to the detector.

As the light intensity of the recombined beam is recorded at the detector, the moveable mirror travels towards the beamsplitter, producing an interferogram.

Fourier-Transform IR

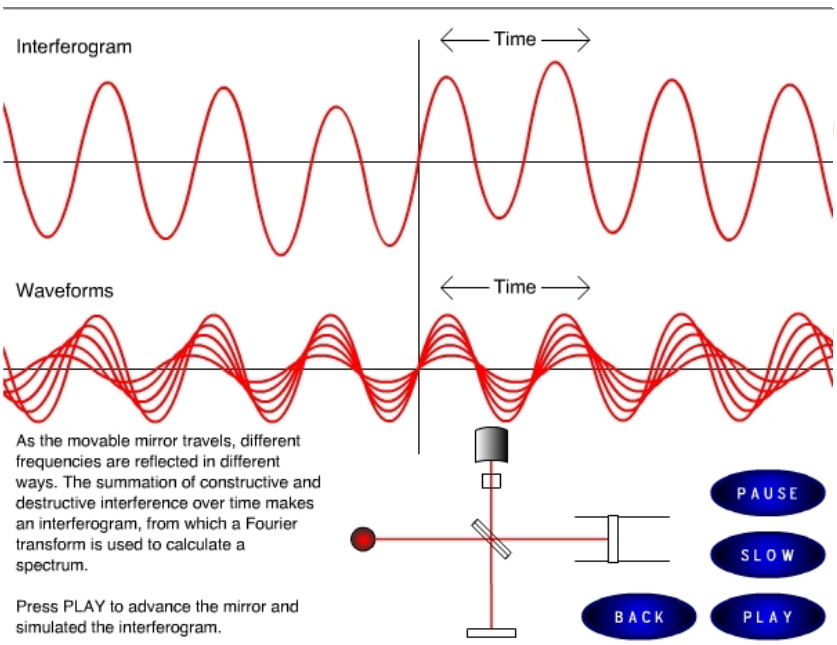

Raman basics

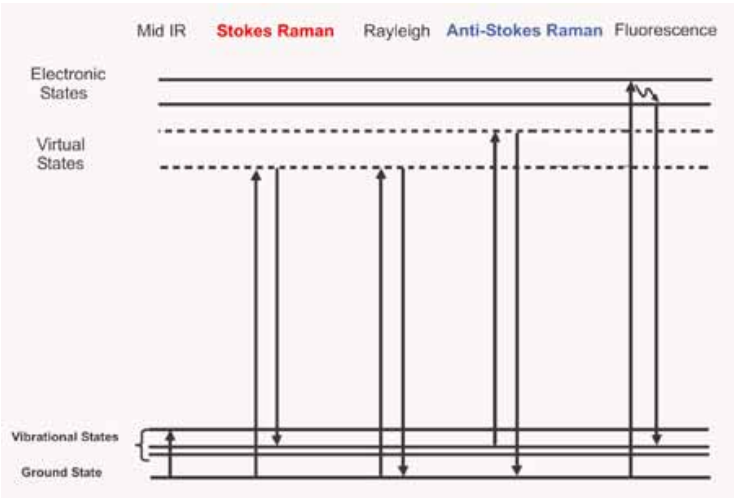

Rayleigh scattering: scattering without change of frequency
Stokes Raman (fraction ca. $1x10^{-7}$): scattering with lower frequency
Anti-Stokes Raman (weaker still): scattering with higher frequency

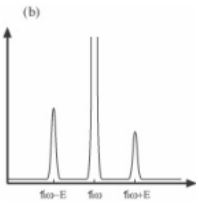

(depends on vibrational state of molecule, i.e. certain selection rules apply)

Enhancement of Raman

Resonant Raman - laser wavelength close to absorption wavelength

SERS or SERRS (surface enhanced (resonance) Raman spectroscopy) - requires a further moiety to be present (eg. a surface or colloid). The presence of such an agent can provide quite dramatic enhancements and has been used successfully in the study of biological samples such as DNA, peptides and proteins.

Active substrates -a substrate with a special coating that concentrates the sample

http://www.jobinyvon.com/usadivisions/Raman/tutorial1.htm

Typical IR spectrum

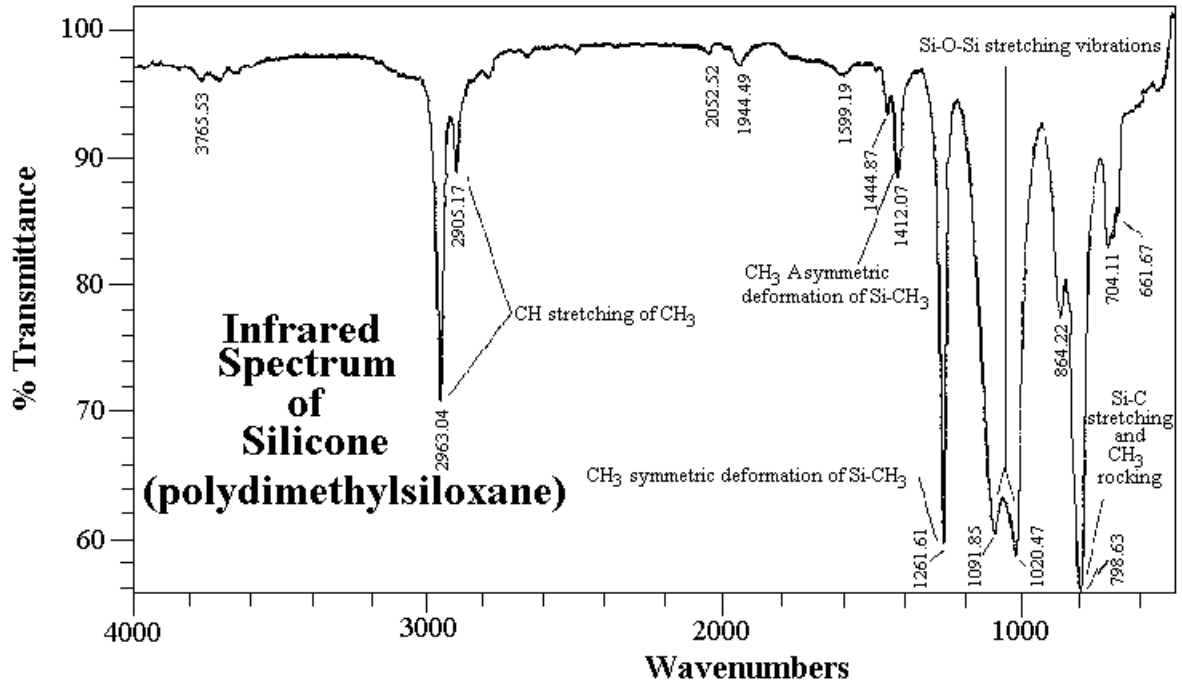

Typical Raman spectrum

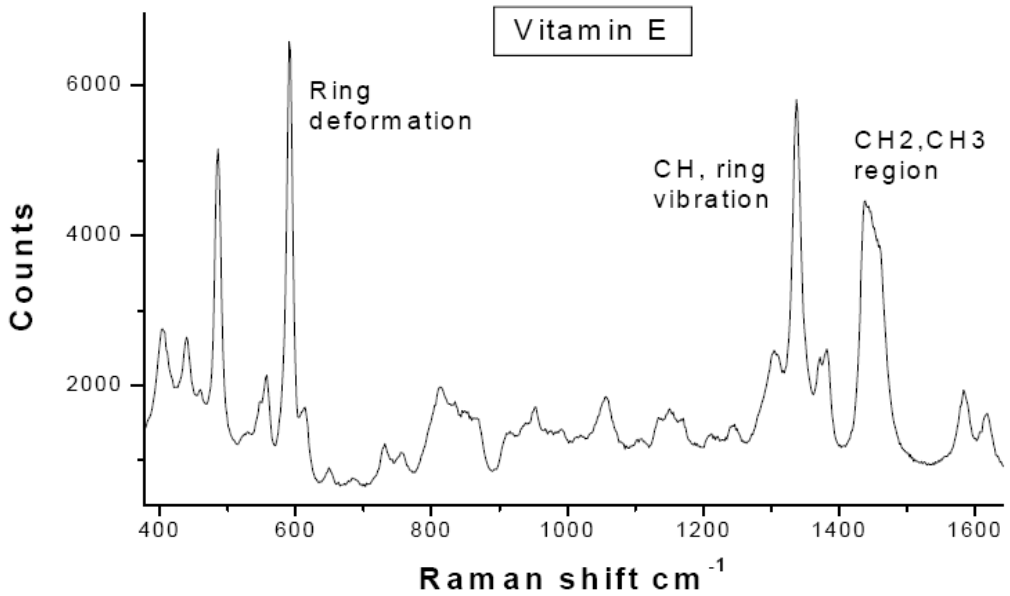

Raman spectrum of vitamin E in solution (97%). The spectrum contains several vibrational frequencies each corresponding to certain molecular bonds. Aquisition time: 30 sec; laser power: 15 mW; confocal Raman microscope

Source: Y. Aksenov, PhD thesis, University of Twente

Bands in IR and Raman spectra of organic molecules

Functional Group/ Vibration	Region	Raman	InfraRed
Lattice vibrations in crystals, LA modes	10 - 200 cm^{-1}	strong	strong
δ(CC) aliphatic chains	250 - 400 cm^{-1}	strong	weak
ν(Se-Se)	290 -330 cm^{-1}	strong	weak
ν(S-S)	430 -550 cm^{-1}	strong	weak
ν(Si-O-Si)	450 -550 cm^{-1}	strong	weak
ν(Xmetal-O)	150-450 cm^{-1}	strong	med-weak
ν(C-I)	480 - 660 cm^{-1}	strong	strong
ν(C-Br)	500 - 700 cm^{-1}	strong	strong
ν(C-Cl)	550 - 800 cm^{-1}	strong	strong
ν(C-S) aliphatic	630 - 790 cm^{-1}	strong	medium
ν(C-S) aromatic	1080 - 1100 cm^{-1}	strong	medium
ν(O-O)	845 -900 cm^{-1}	strong	weak
ν(C-O-C)	800 -970 cm^{-1}	medium	weak
ν(C-O-C) asym	1060 - 1150 cm^{-1}	weak	strong
ν(CC) alicyclic, aliphatic chain vibrations	600 - 1300 cm^{-1}	medium	Medium
ν(C=S)	1000 - 1250 cm^{-1}	strong	weak
ν(CC) aromatic ring chain vibrations	*1580, 1600 cm^{-1}	strong	medium
	*1450, 1500 cm^{-1}	medium	medium
	*1000 cm^{-1}	strong/medium	weak
δ(CH3)	1380 cm^{-1}	medium	strong
δ(CH2) δ(CH3) asym	1400 - 1470 cm^{-1}	medium	medium
δ(CH2) δ(CH3) asym	1400 - 1470 cm^{-1}	medium	medium
ν(C-(NO2))	1340 - 1380 cm^{-1}	strong	medium
ν(C-(NO2)) asym	1530 - 1590 cm^{-1}	medium	strong
ν(N=N) aromatic	1410 - 1440 cm^{-1}	medium	-
ν(N=N) aliphatic	1550 - 1580 cm^{-1}	medium	-
δ(H2O)	~1640 cm^{-1}	weak broad	strong
ν(C=N)	1610 - 1680 cm^{-1}	strong	medium
ν(C=C)	1500 - 1900 cm^{-1}	strong	weak
ν(C=O)	1680 - 1820 cm^{-1}	medium	strong
ν(C≡C)	2100 - 2250 cm^{-1}	strong	weak
ν(C≡N)	2220 - 2255 cm^{-1}	medium	strong
ν(-S-H)	2550 - 2600 cm^{-1}	strong	weak
ν(C-H)	2800 - 3000 cm^{-1}	strong	strong
ν(=(C-H))	3000 - 3100 cm^{-1}	strong	medium
ν(≡(C-H))	3300 cm^{-1}	weak	strong
ν(N-H)	3300 - 3500 cm^{-1}	medium	medium
ν(O-H)	3100 - 3650 cm^{-1}	weak	strong

Source: HORIBA Jobin Yvon

MESA+

University of Twente
The Netherlands

MESA+

University of Twente
The Netherlands

Instrumentation

A few examples

Raman -how it began

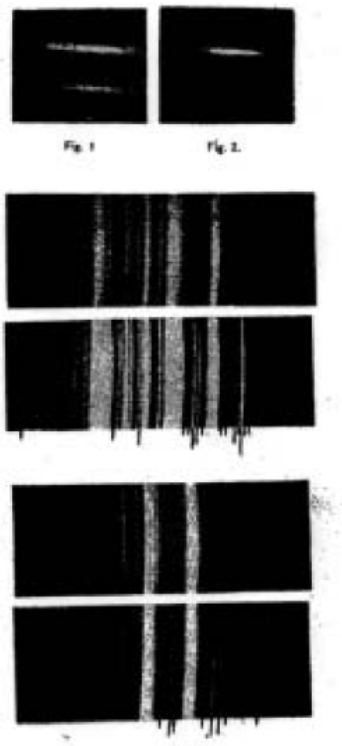

Above: Raman's spectrograph with photographic plate
Right: First spectra published in Indian Journal of Physics

1922-1927: molecular light scattering predictions by Raman, Smekal, Kramers and Heisenberg, Cabannes and Daure, Rocard, and Schroedinger and Dirac

1928: C.V. Raman reports the effect; first he used filtered sunlight, a prism spectroscope, and visual observation, later filtered Hg light and a photographic plate

MESA+

University of Twente
The Netherlands

Spectrometers in the 1940's and 1950's

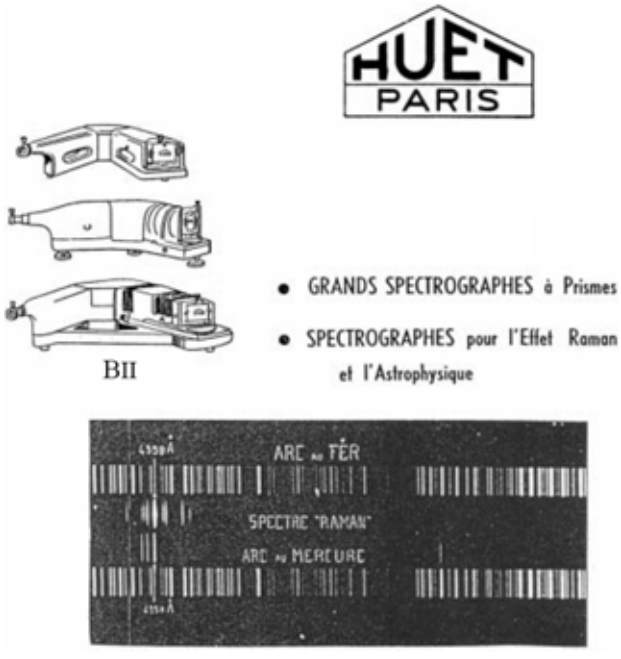

Huet prism (35 cm)spectrometer -1940's

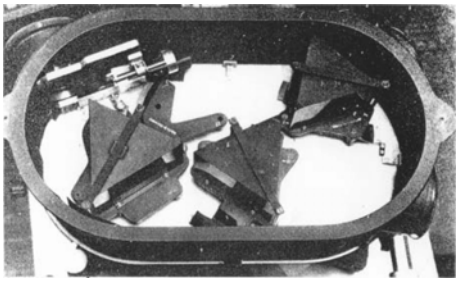

3-4 cm prisms in Steinheil Raman Spectrometer-1957

MESA+

Source: www.jobinyvon.com

University of Twente
The Netherlands

50 years down the line

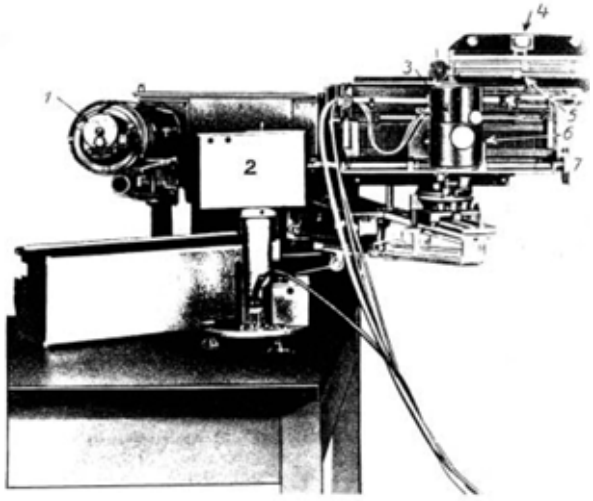

Steinheil Raman Spectrometer-1957

Horiba Raman Spectrograph with multiplexing capability for on-line industrial process monitoring-2005

Horiba inverted microscope with Raman Spectrometer-2005

MESA+

Source: www.jobinyvon.com

University of Twente
The Netherlands

MESA+

University of Twente
The Netherlands

IR and Raman generated by a chip

InfraRed lasers/LEDs and photodiodes

Photodiode (9 mm size)
(1000-3600 nm)

IR laser diode
(735 nm - 3.8 µm)

IR LEDs (850 - 940nm)
Sizes 3 -8mm

MESA+

University of Twente
The Netherlands

Silicon Raman Lasers

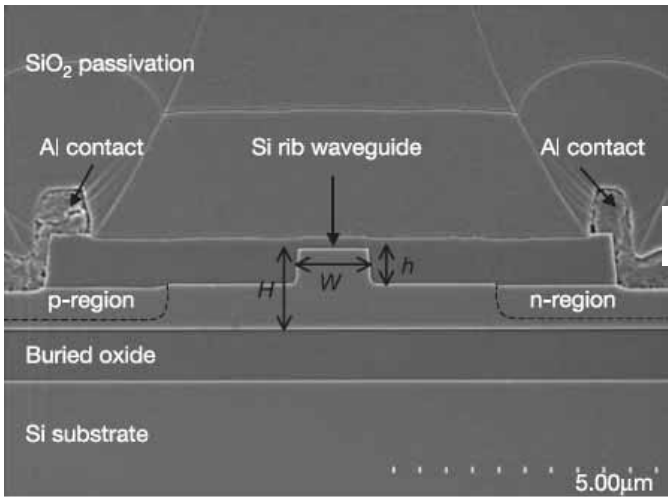

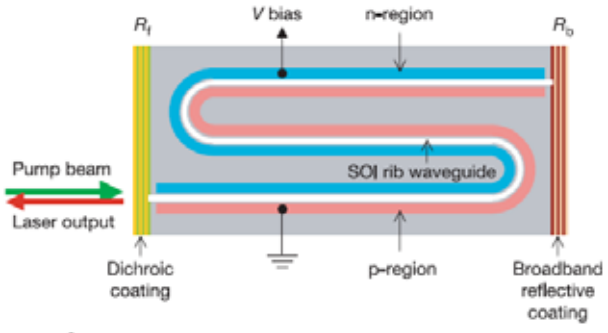

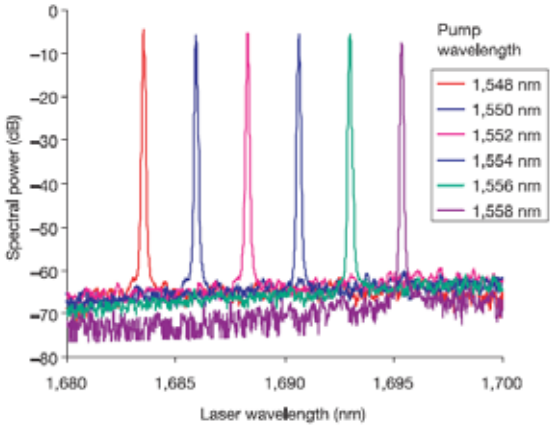

MESA+

Rong e.a. Nature 433, 725-728 (2005) & 433, 292-294 (2005)

University of Twente
The Netherlands

More Raman laser microdevices

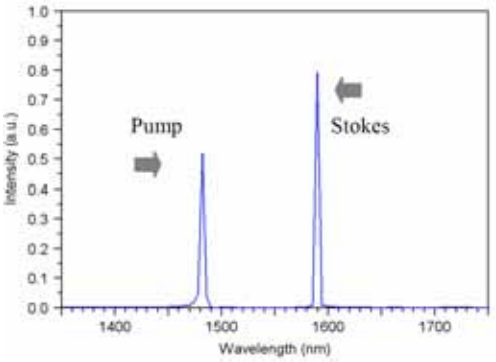

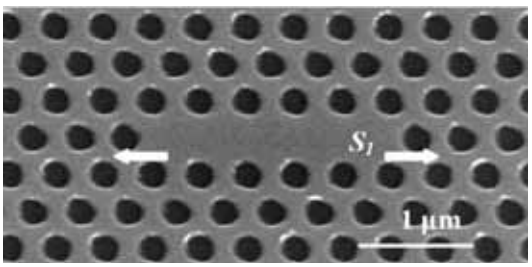

Silicon photonic crystal Raman laser
Yang e.a. Optics Express 13, 4723-4730 (2005)

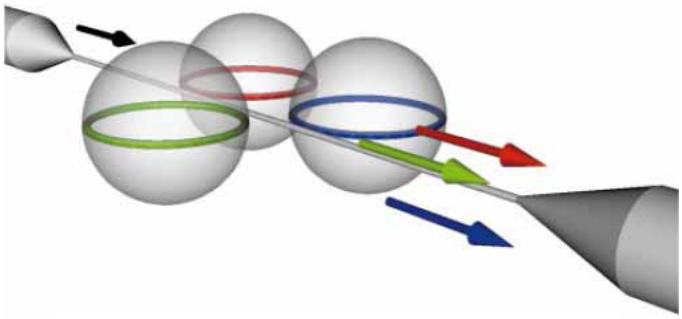

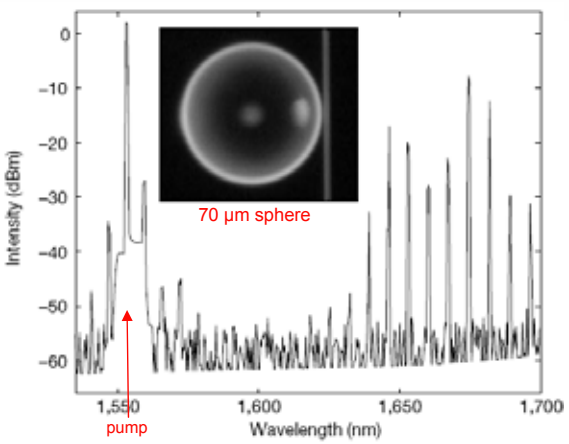

Silica microsphere Raman laser
Spillane e.a Nature 415, 621-623 (2002)

IR and Raman measured by a chip

InfraRed detectors

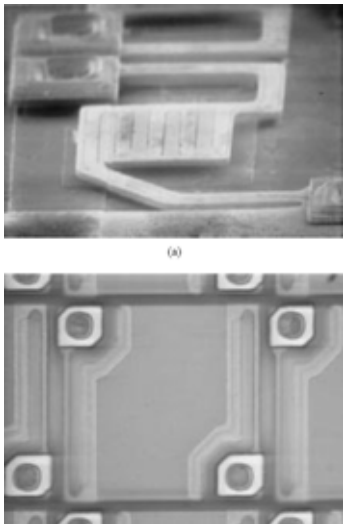

Top: microemitter pixel
Bottom: microbolometer (IR-sensor) pixel
Both are on 50 µm pitch

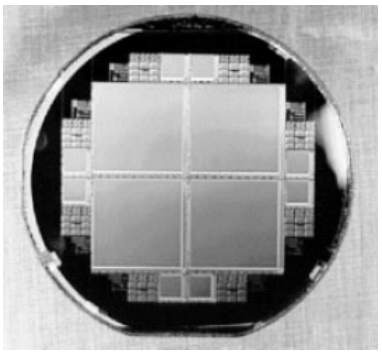

4" substrate with four 512x512 microemitter pixel arrays

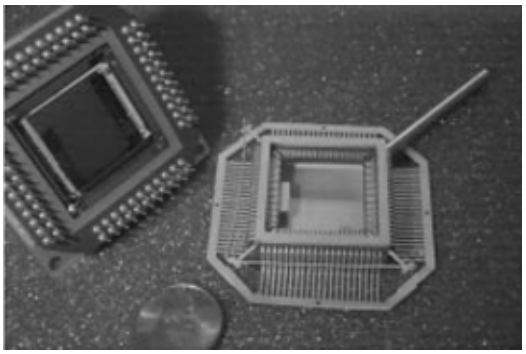

Ceramic vacuum package

IR image with 240x336 microbolometer camera

Cole e.a. Proc. IEEE 86, 1679-1686 (1998)

MESA+

University of Twente
The Netherlands

MESA+

University of Twente
The Netherlands

IR and Raman measured on a microfluidic chip

On-line FT-IR detection on CE chips

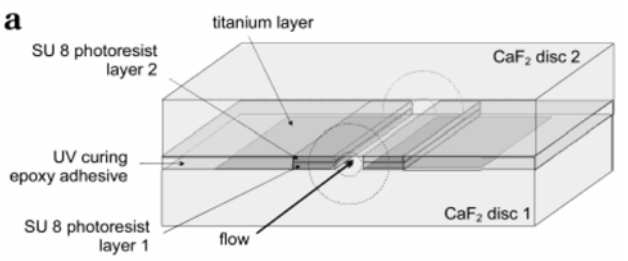

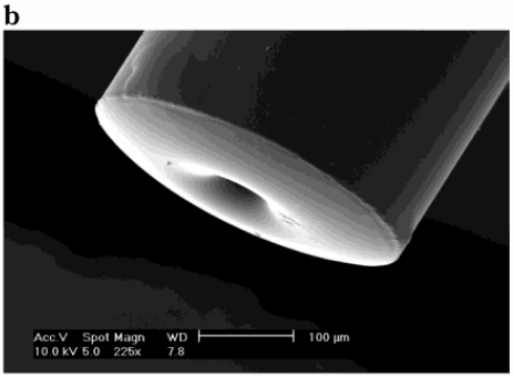

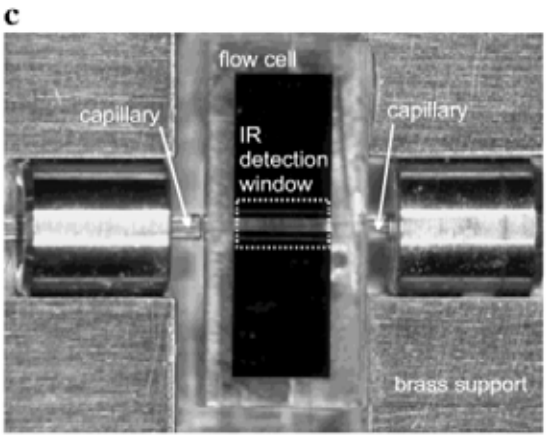

(a) Schematic view of the CE-FT-IR cell
(b) SEM micrograph of capillary O-ring
(c) Microscopic view of the CE-FT-IR cell, with connected capillaries, housed in supporting block

Kölhed e.a. Anal.Chem. 74, 3843-4848 (2002)

CaF_2 CE chips

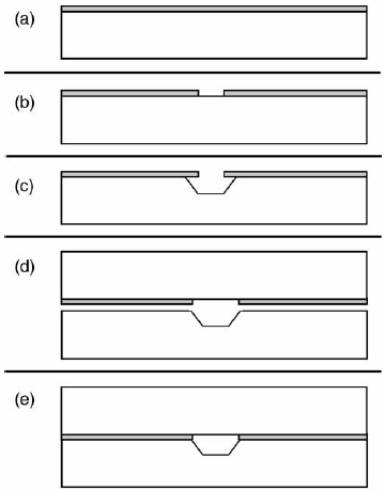

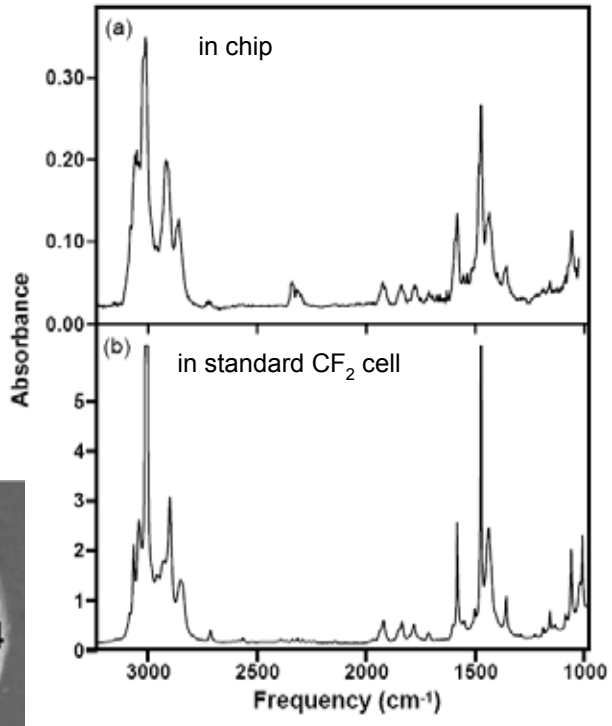

etching in saturated aqueous $Fe(NH_4)(SO_4)_2$ solution at 18 µm/day; bonding with photoresist (also serves as optical filter), in oven at 135 ◦C for 30 min

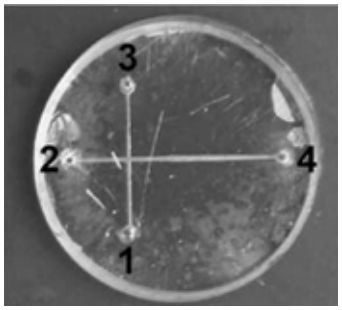

Pan e.a. J.Chrom.A 1027, 231-235 (2004)

Diffusional IR mixer

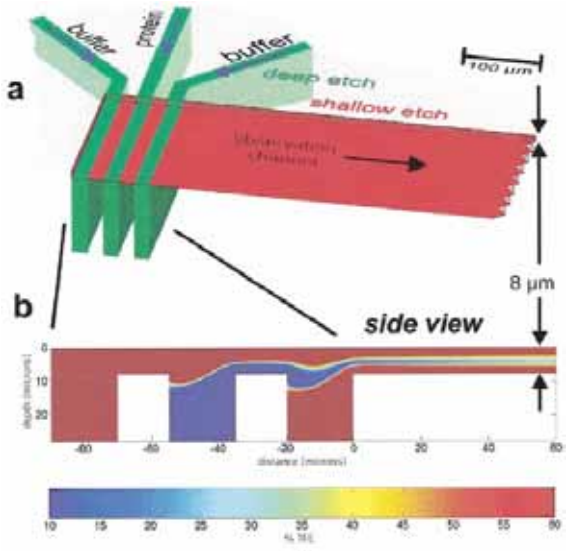

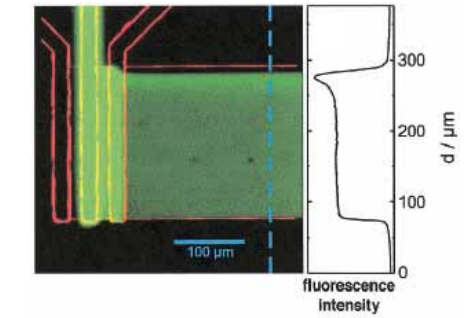

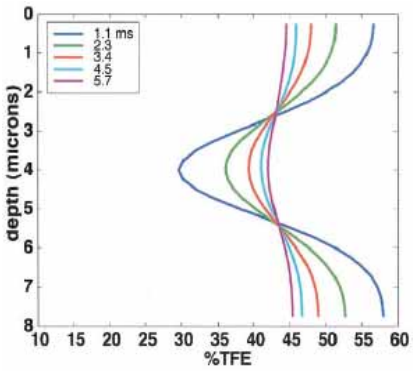

Study of the lifetimes of intermediates in the β-sheet to α-helix transition of β-lactoglobulin; time resolution is achieved by scanning along the observation channel with the focused beam of an FTIR microscope (see next slide)

Kauffmann e.a. PNAS 98, 6646-6649 (2001)

FTIR microscope

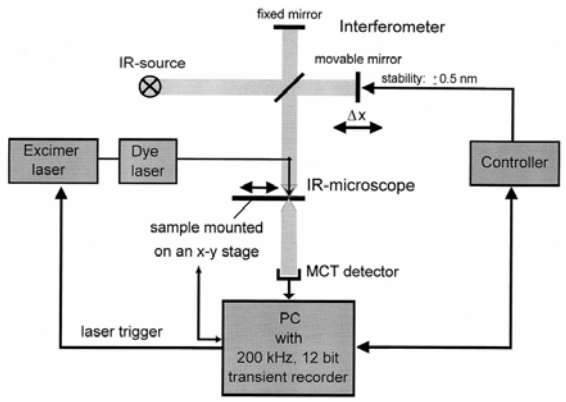

Rammelsberg e.a. Vibr.Spectr. 19, 143-149 (1999)

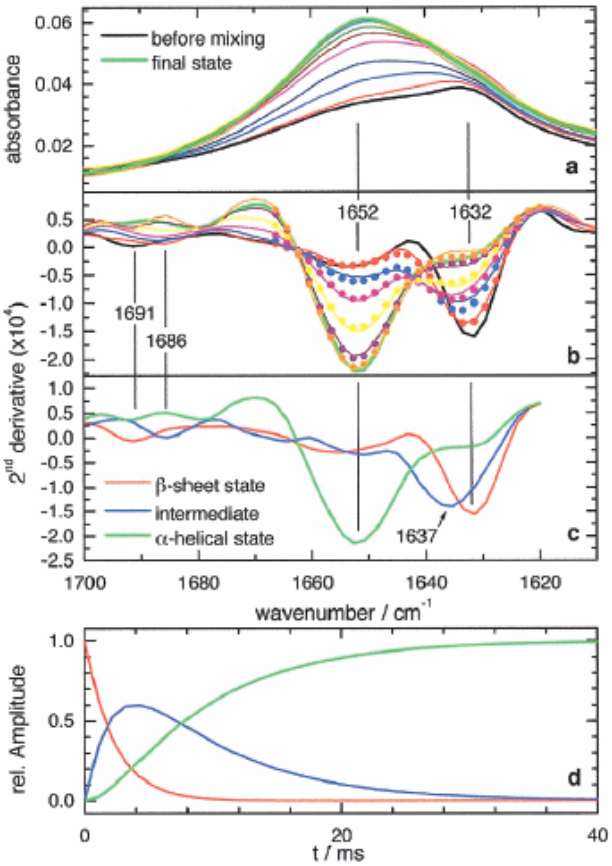

Time-resolved FTIR spectra and kinetic analysis
a) spectra taken along the observation channel, at 1.1, 3.4, 5.7, 10.2, 21.6, and 103 ms; black line: before mixing, green line: final state
b) 2nd derivative spectra of a) with three-state exp. fits (dots); basic spectra are shown in c).
d) Time course of the 3 states as deduced from the fit

Kauffmann e.a. PNAS 98, 6646-6649 (2001)

Photoacoustic detection on a chip

Principle of photoacoustic spectroscopy:

incident light is modulated at an acoustic frequency. If the optical wavelength couples to an energy transition in the gas, the gas absorbs the light resulting in a periodic gas expansion that can be detected by a microphone

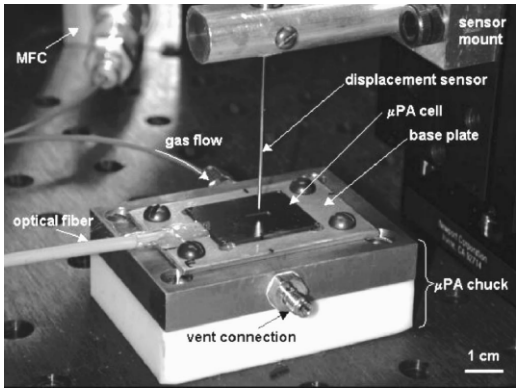

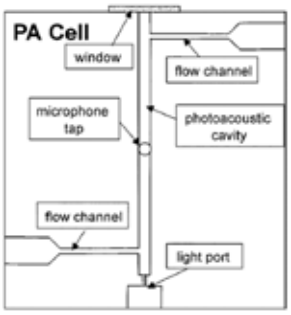

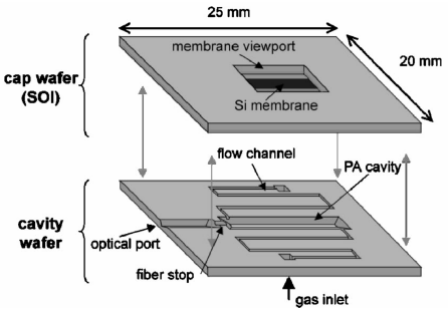

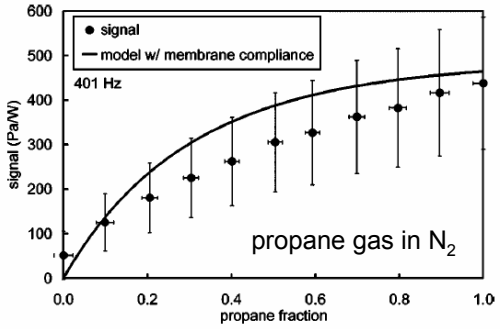

Firebaugh e.a. J.Appl.Phys. 92, 1555-1563 (2002)

Attenuated Total (Internal) Reflection

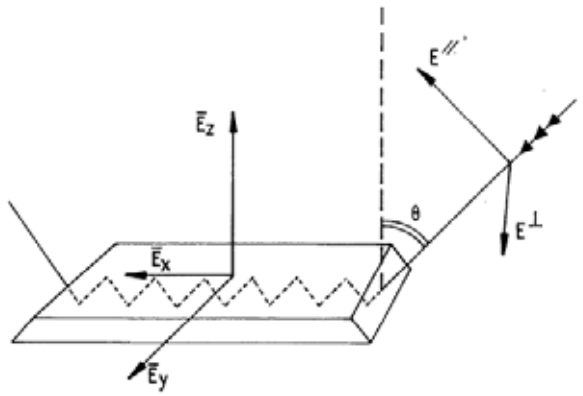

Principle:

IR beam is directed into high refractive index medium which is transparent for IR radiation. Above critical angle θc the light beam is completely reflected at the surface. Multiple internal total reflections occur

$$\theta_c = \sin^{-1}\left(\frac{n_2}{n_1}\right)$$

Evanescent wave amplitude:

$$E = E_0 \exp\left(\frac{-z}{d_p}\right)$$

Evanescent field penetration depth:

$$d_p = \frac{\lambda}{2\pi n_1 \sqrt{\sin^2\theta - \left(\frac{n_2}{n_1}\right)^2}}$$

Effective penetration depth for absorbance:

$$d_e = \frac{n_2 E_0^2 d_p}{n_1 \cos\theta}$$

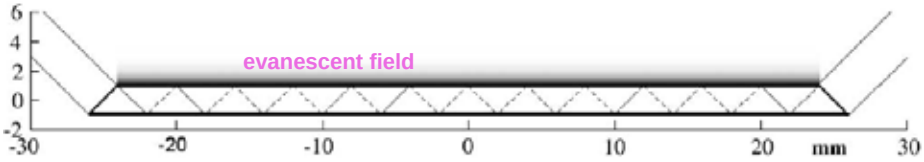

More details in: Vigano e.a. Talanta 65, 1132-1142 (2005)

Optical and physical properties of materials

Materials	n_1	θ_c (°) in water	Hardness (kg/mm^2)	Wavelength range	Comments	θ (°)	d_e (μm)	d_p (μm)
Ge	4.0	22	780	4000–830	Stable in water, in acids and alkalis attacked by hot H_2SO_4	30	1.92	0.73
						45	0.74	0.40
						60	0.39	0.31
Si	3.4	26	1150	4000–1500	Stable in water, in acids and alkalis attacked by HF and HNO_3	30	4.32	1.17
						45	1.17	0.51
						60	0.59	0.38
ZnSe	2.4	39	120	4000–650	Stable in water pH 5–9	45	5.29	1.22
						60	1.86	0.67
KRS-5	2.4	39	40	4000–400	Not very stable in water	45	5.29	1.22
						60	1.86	0.67
Diamond	2.35	40	Very hard	4000–400	Stable in water pH 1–14	45	6.17	1.35
						60	2.03	1.69
ZnS	2.2	43	355	4000–950	Stable in water, not at acidic pH	45	12.65	2.34
						60	2.75	0.82

Other materials such as CdTe ($n_1 = 2.65$, hardness = 45) are close to those described in the table. The values of the efficient penetration depth of the evanescent wave have been calculated at a wavelength of 1650 cm^{-1} for a randomly polarized light. The critical angle is calculated in water ($n = 1.5$). KRS-5 is a thallium bromide/thallium iodide eutectic.

Vigano e.a. Talanta 65 1132-1142 (2005)

ATR on microchannels

Characterization of Protein Adsorption and Immunosorption Kinetics in Photoablated Polymer Microchannels

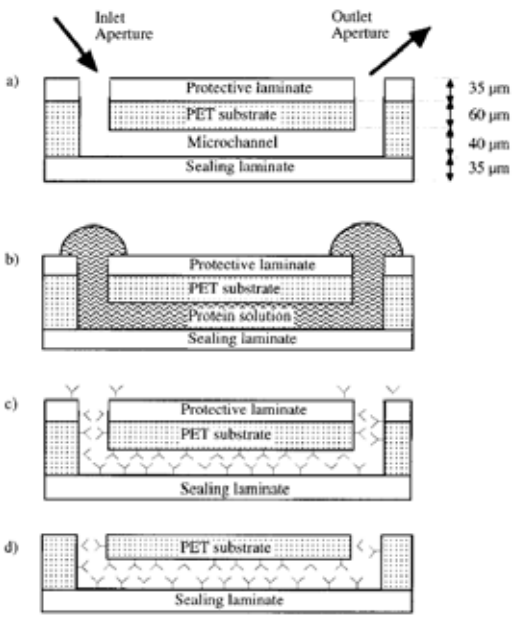

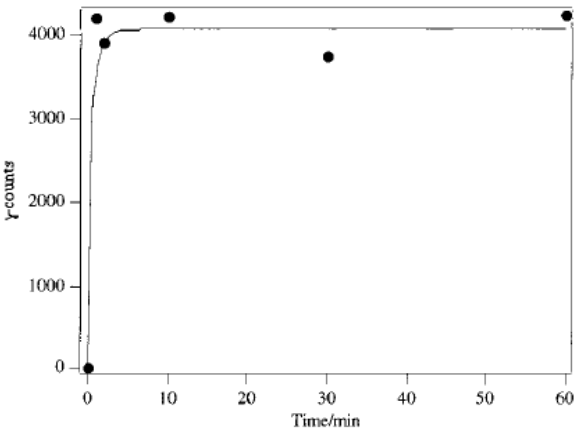

Adsorption kinetics of SEB in a photoablated microchannel. The channel was incubated with 3.12nMof anti-SEB for 1 hr whereas the solution of SEB was incubated at 36 nM between 1 and 60 min and revealed by the secondary radiolabeled anti-SEB at 200 nM.

Rossier e.a. Langmuir 16, 8489-8494 (2000)

Extension of IR bandwidth in Si ATR

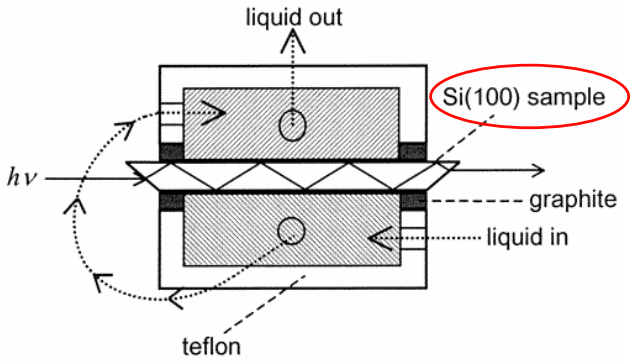

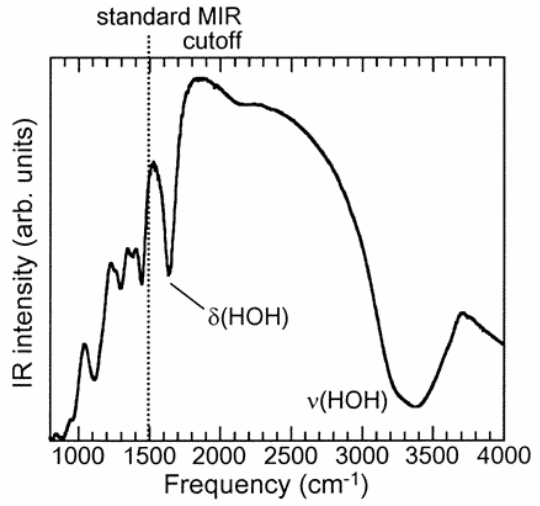

The use of Si(100) allows shorter samples, thus less absorbance in the Si (bandwidth is limited by multiphonon bands that effectively absorb all the incident IR radiation below 1500 cm^{-1})

NB MIR (Multiple Internal Reflection) = ATR

Queeney e.a. J.Phys.Chem.B 105, 3903-3907 (2001)

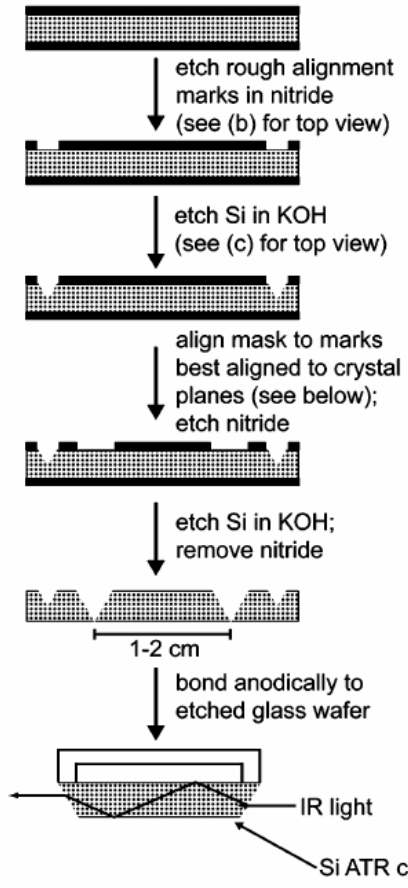

Infrared spectroscopy for chemically specific sensing in silicon-based microreactors

Alignment to <110> directions
(needed for ATR inlet aperture)

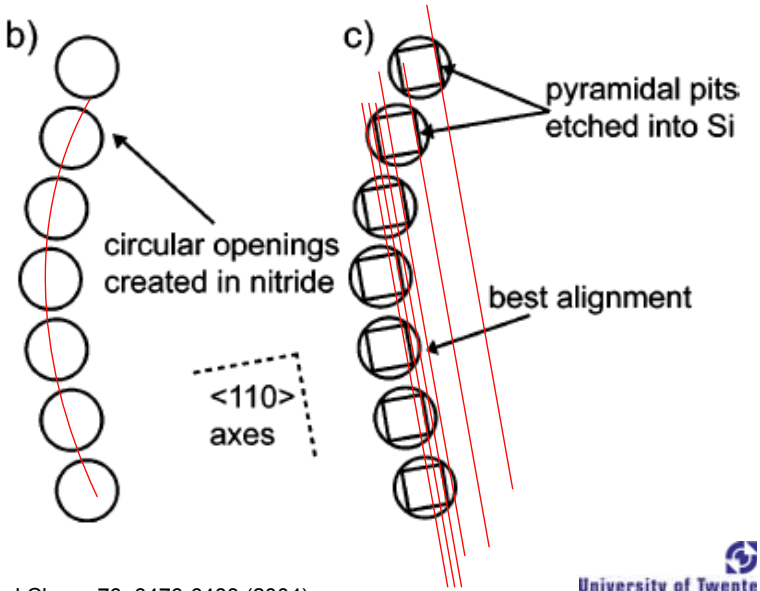

Herzig-Marx e.a. Anal.Chem. 76, 6476-6483 (2004)

Infrared spectroscopy for chemically specific sensing in silicon-based microreactors

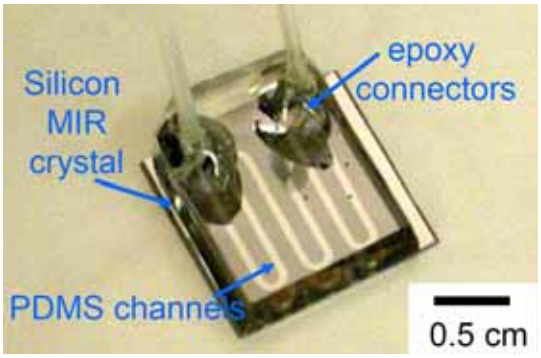

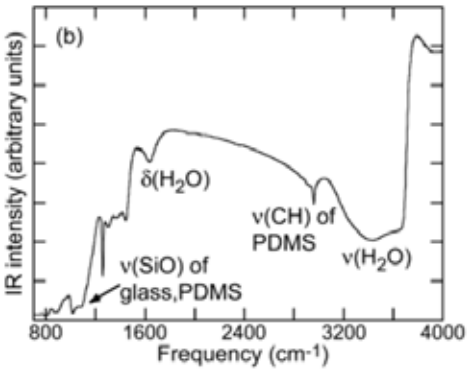

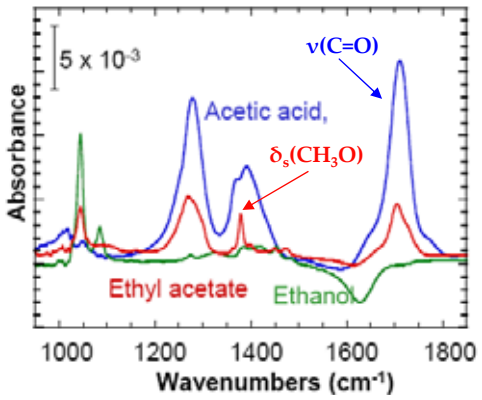

Infrared spectra (100 scans) of reactants and products of ethyl acetate hydrolysis, acquired in aqueous solution (5 ml/100 ml H_2O) in a microreactor

Herzig-Marx e.a. Anal.Chem. 76, 6476-6483 (2004)

Silicon micromixers with IR detection

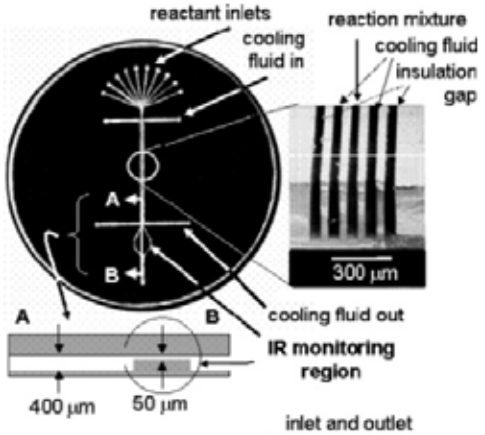

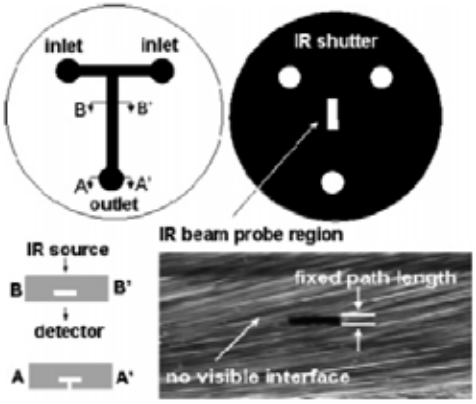

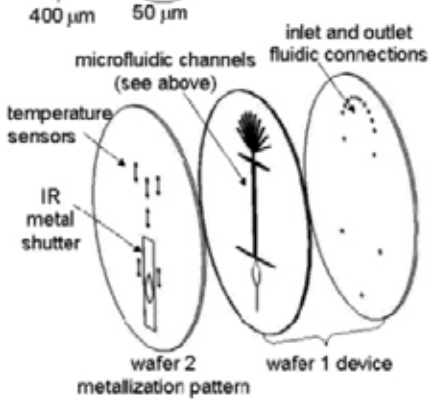

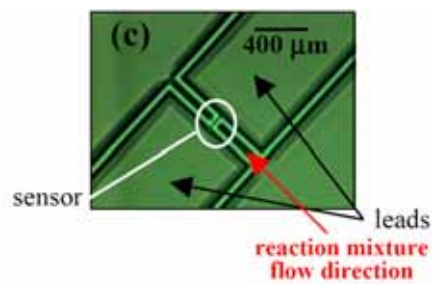

Floyd e.a. Ind.Eng.Chem.Res. 44, 2351-2358 (2005)

Micromixer simulation and testing

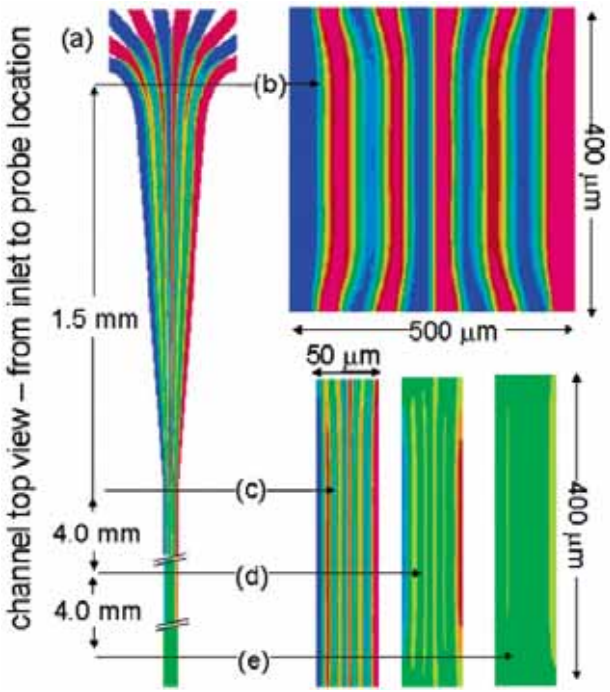

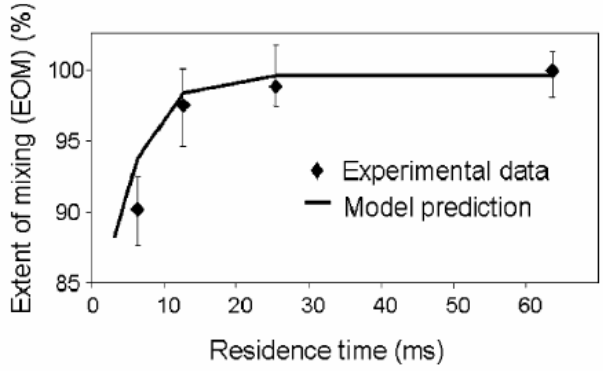

Floyd e.a. Ind.Eng.Chem.Res. 44, 2351-2358 (2005)

Silicon micromixers with IR detection

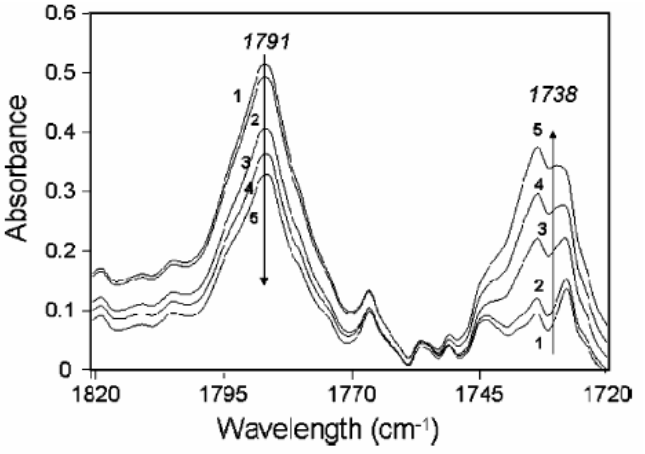

FTIR data of the progress of hydrolysis of propionyl chloride: (1) 2.4 s, (2) 4.9 s, (3) 48.6 s, (4) 81 s, and (5) 243 s, 0.4 M propionyl chloride at 23 °C.

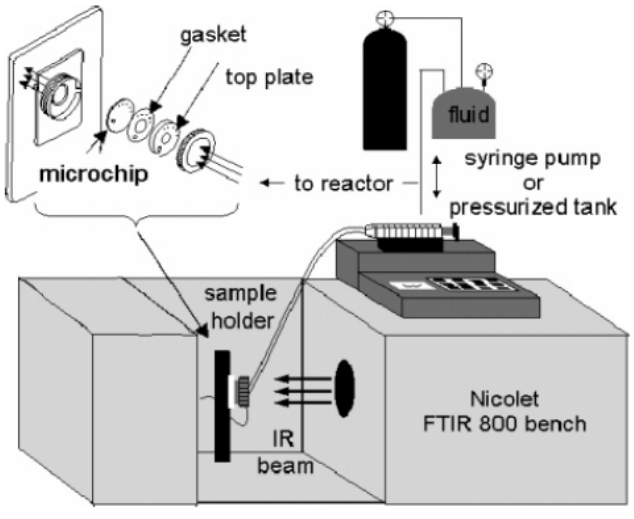

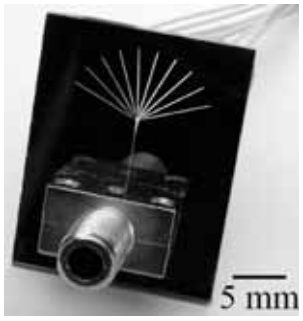

Floyd e.a. Ind.Eng.Chem.Res. 44, 2351-2358 (2005)

Microreactors with Raman microspectrometry

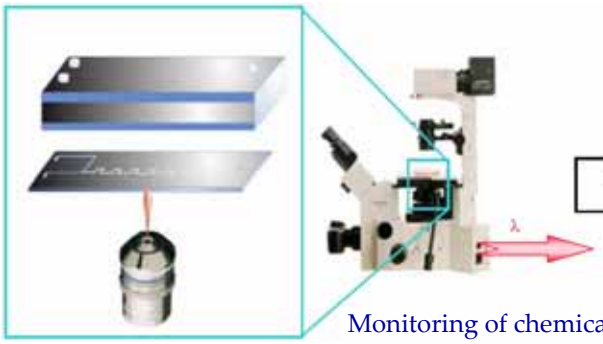

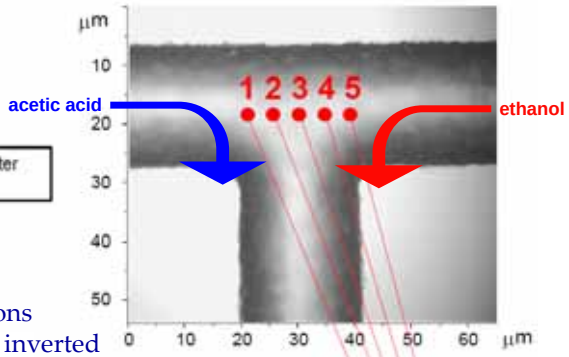

Monitoring of chemical reactions within microreactors using an inverted Raman microscopic spectrometer

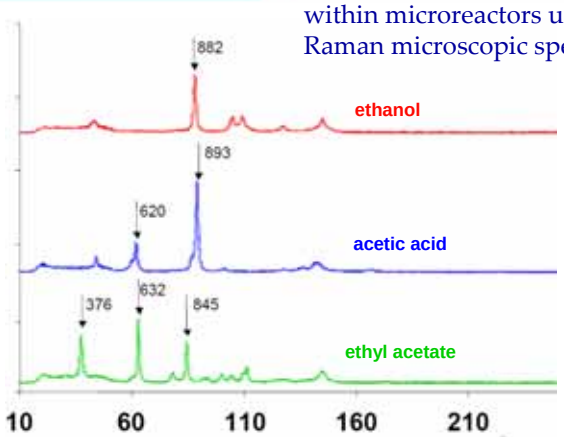

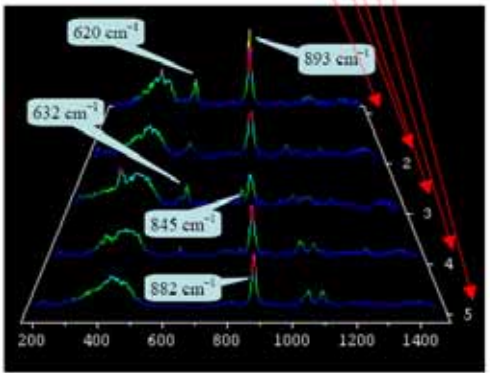

MESA+

Fletcher e.a. Electrophoresis 24, 3239–3245 (2003)

University of Twente The Netherlands

Surface enhanced Raman on a chip

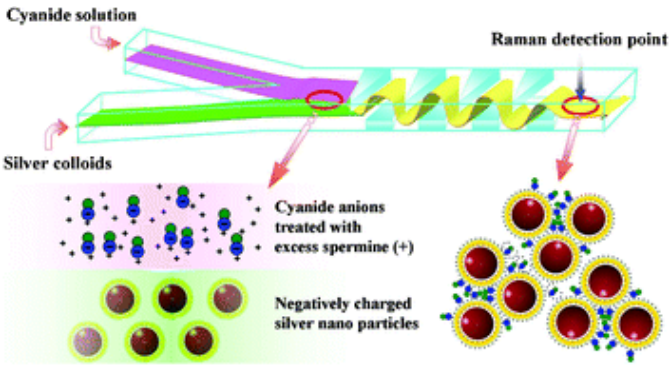

Ultra-sensitive trace analysis of cyanide water pollutant in a PDMS microfluidic channel using confoccal surface-enhanced Raman spectroscopy

"Alligator teeth-shaped" microfluidic mixer

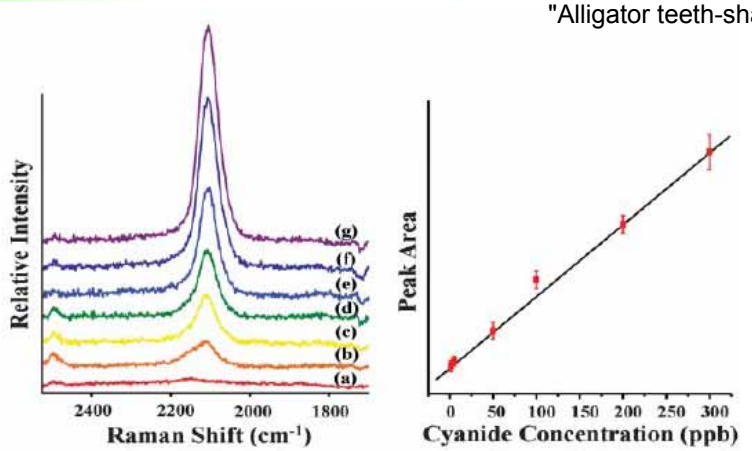

MESA+

Yea e.a. Analyst 130, 1009-1011 (2005) & Lab Chip 5, 437-442 (2005)

University of Twente The Netherlands

Raman microspectroscopy on cells

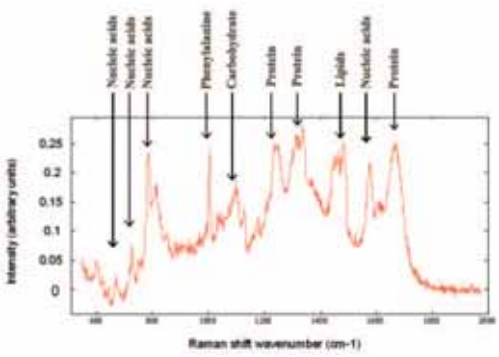

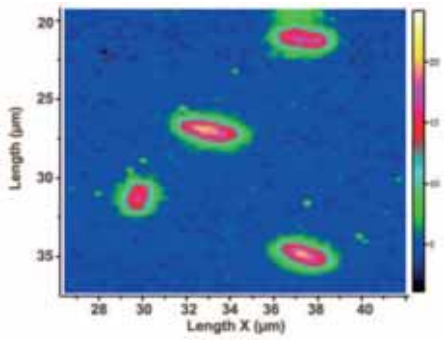

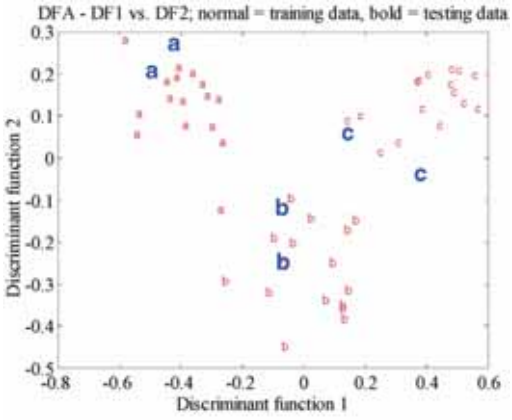

Top left: Typical Raman spectrum acquired from a single cell of size 1-2 μm

Top right: Raman mapped image of four bacteria cells

Bottom right: Multivariate analysis of spectra from three bacterial species showing good discrimination between species

From Bioforum Europe 9(4), 56-57 (2005) ; details: Huang e.a. Anal.Chem. 76, 4452-4458, 2004

Raman microspectroscopy on cells in a chip

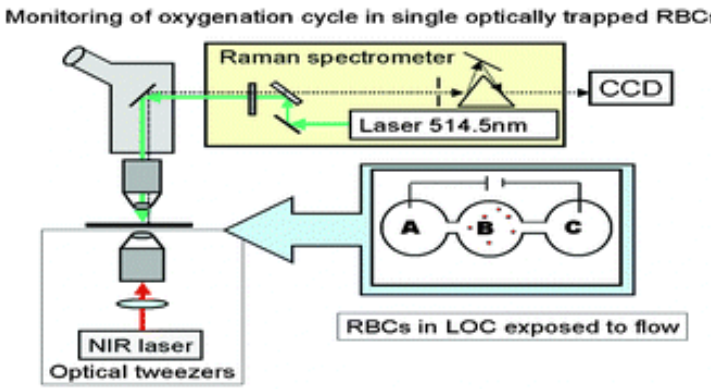

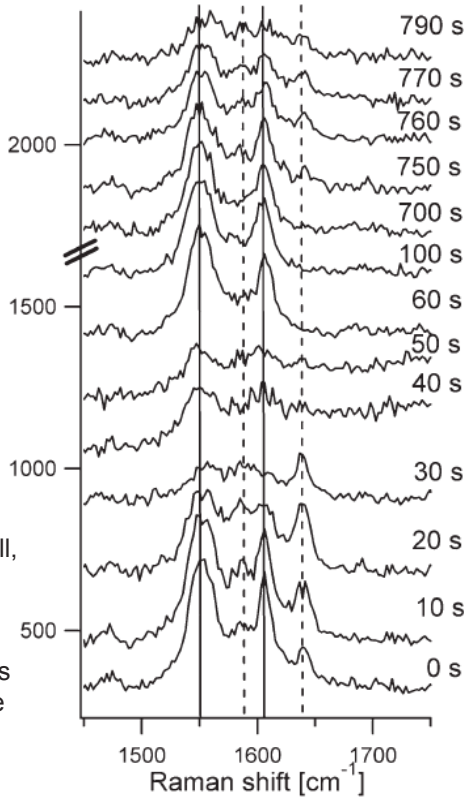

Right: Oxygenation cycle of single optically trapped red blood cell, exposed to constant Hepes buffer flow.
After 40 s sodium dithionite is added to chamber A and transported to the RBC through EOF. Next, fresh Hepes buffer was flushed through the reservoir and after ~750 s the RBC turns into a mixed oxy–deoxyHb state again before finally reaching the inactive metHb state after 790 s

Ramser e.a. Lab Chip 5, 431-436 (2005)

Rorschach inkblot test

or

InfraRed image?

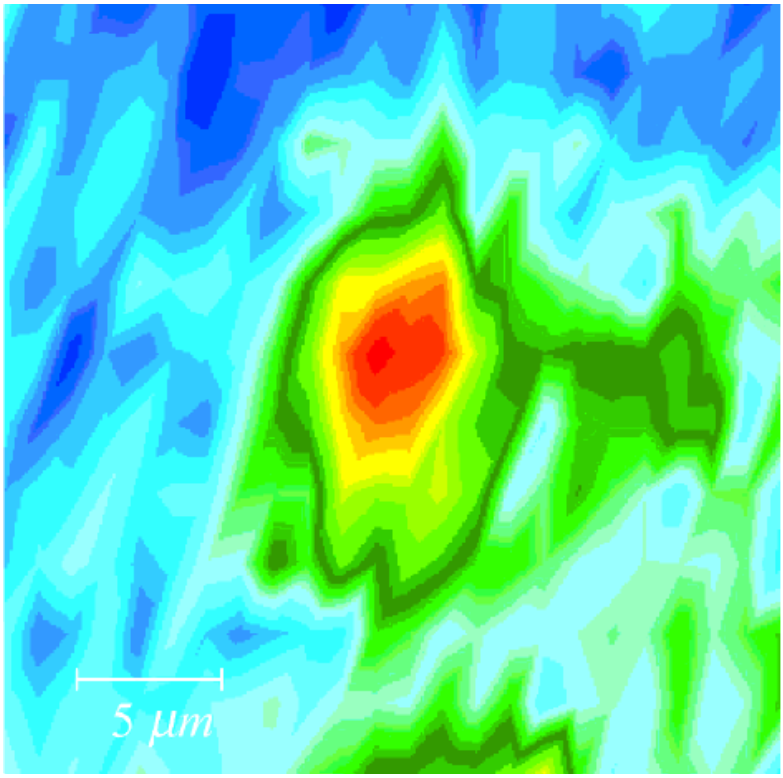

ATIR Infrared image of a single red blood cell
Sommer e.a. Appl.Spectr. 55, 252-256 (2001)